 ICCES, vol.13, no.1, pp.15-21

A meshless model for rapid prediction of indoor contaminant dispersion

Darrell W. Pepper[1], Xiuling Wang[2]

Summary

A meshless method for simulating indoor contaminant dispersion within buildings and rooms has been developed. The approach utilizes the advantages of the meshless method by distributing collocation points and different order radial basis functions according to the computational domain and evolving numerical solution. The numerical scheme yields fast convergence and high accuracy necessary for providing quick assessments of contamination transport within enclosures.

Introduction

Mesh-free methods have the following advantages: (1) they require neither domain nor boundary discretization; (2) domain integration is not required; (3) they converge exponentially for smooth boundary shapes and boundary data; (4) they are attractive to high dimensional problems; and (5) implementation and coding are very easy. By coupling the meshless method with a Lagrangian particle technique, contaminant transport can be quickly and accurately simulated and graphically displayed. The model includes the ability to read CAD drawings of a building – permitting quick assessment of offices or rooms on a floor including ventilation pathways. The model is particularly appealing for evaluating contaminant transport as well as risk assessment associated with homeland security issues [1]–[6].

The threat of chemical and biological agents being dispersed within a building has become a reality, and is an important cornerstone of the homeland security initiative and Department of Homeland Security instigated by the US government. This issue became evident when a letter contaminated with anthrax was sent to former Senator Tom Daschle's office in October 2001. Senator Daschle's office resided in the Hart Senate Office Building, which is a 9-story complex located near the Capital Building in Washington, DC. Fumigation and cleanup of the building took approximately three months and cost about $14M. Traces of anthrax were found in other rooms; however, it is unknown exactly how the aerosolized spores dispersed from the envelope to other parts of the building.

One gram of anthrax contains about 100 billion spores. Only about 10,000 spores are needed to generate a lethal dose attributed to inhalation. Anthrax ranges in size from 2-4 microns – a fairly large aerosol – which makes the spores susceptible to gravitational settling. This means that anthrax can quickly settle onto carpets, tabletops, desktops, keyboards, etc. Generally smaller aerosols tend to adhere to ceilings and walls. Assuming someone inadvertently opens an envelope

[1]Dept. of Mech. Engr., UNLV, 4505 Maryland Pkwy, Las Vegas, NV 89154-4027
[2]Dept. of Mech. Engr., Purdue University Calumet, Hammond, IN, 46323

containing one gram of anthrax, some of the anthrax will remain in the envelope, some will settle onto the floor, some will become dispersed into the air, and some may likely be deposited onto and into the person opening the letter. Since people move from room to room, the anthrax will likely be tracked, resuspended, and re-deposited within the facility. In addition, the air circulation and HVAC will aid in the redistribution of the spores through the vents and ducts.

Potential Hazards

Delivery methods vary for introducing chemical and biological agents, e.g., non-exploding means such as open gas cylinders, open containers of liquid agents left to evaporate aerosol generators, spray tanks, and dry powder. Explosive means vary from gigantic eruptions to small explosive charges.

Chemical agents tend to degrade or disperse in a few hours to a few weeks when exposed to the elements. Biological agents are either in viral or bacterial forms. Viruses range from 0.01-0.30 microns while bacteria range from 0.3-35 microns in diameter. Typical examples of biological agents are anthrax, botulism, plague, smallpox, tularemia, and hemorrhagic fever (for which there are over 12 types of viruses).

While biological agents typically will not cause immediate symptoms, chemical agents almost always cause immediate symptoms. An example of the immediate effects of chemical weapons was evident during World War I when mustard gas was released and dispersed into the trenches, affecting thousands of soldiers. Similar effects were felt by US troops during the Vietnam War in the 1960's when agent orange was dropped as a defoliating agent. Saddam Hussain used chemical agents in Iraq following the Gulf War of 1991 in a genocide that killed thousands of Kurds. The invasion of Iraq in 2003 by the US was based on the premise that Iraq was stockpiling weapons of mass destruction including biological and chemical agents.

Terrorists seek to promote fear and confusion by selecting targets of opportunity where people generally feel safe, e.g., shopping malls, sporting events, churches, and major performances. The September 11, 2001 World Trade Center disaster clearly illustrated the risks and consequences of terrorist attacks on buildings that can hold over 50,000 people. Terrorists' incidents have numbered in the thousands in some countries. Recent incidents indicate a dramatic shift of terrorist ideology towards mass destruction and global visibility.

Classrooms, auditoriums, and public buildings tend to have transient or variable occupancy. Ventilation rates in these enclosures are typically varied to maintain acceptable contaminant concentrations at all times. A pollutant can be indoors before the start of occupancy, produced by people, processes or materials placed within the building, or supplied from the outside through exterior ventilation.

Model Description

Radial basis functions (RBFs) are increasingly being used as an alternative to traditional discretization schemes employed in finite difference/finite volume/finite element methods. A major advantage with using RBFs is that the nodal points do not need to be uniform in anyway. A random scattering of data points can be used just as easily as a uniform grid. One of the most popular choices for RBFs is the multiquadrics (MQ) approximation [7] [9][10]. A function is first approximated by an RBF, and its derivatives are then obtained by differentiating the RBF.

Since multiquadrics (MQ) are infinitely smooth functions, they are often chosen as the trial function for ϕ (some form of RBF), i.e.,

$$\phi(r_j) = \sqrt{r_j^2 + c^2} = \sqrt{(x-x_j)^2 + (y-y_j)^2 + c^2} \tag{1}$$

where c is a shape parameter provided by the user (Kansa, 1990).

The equations associated with fluid flow and species transport can be discretized using a linear combination of RBFs and expressed in the forms [13]

$$\sum_{j=1}^{N} \hat{V}_j^{n+1} \phi_j(x_i, y_i) = \sum_{j=1}^{N} V_j^n \phi_j(x_i, y_i) + \Delta t \left[\mu \sum_{j=1}^{N} V_j^n \nabla^2 \phi_j(x_i, y_i) - \sum_{j=1}^{N} P_j^n \nabla \phi_j(x_i, y_i) - \sum_{j=1}^{N} V_j^n \phi_j(x_i, y_i) \sum_{j=1}^{N} V_j^n \nabla \phi_j(x_i, y_i) + \sum_{j=1}^{N} B_j^n \phi_j(x_i, y_i) \right] \tag{2}$$

$$\sum_{j=1}^{N} C_j^{n+1} \phi_j(x_i, y_i) = \sum_{j=1}^{N} C_j^n \phi_j(x_i, y_i) + \Delta t \left[D \sum_{j=1}^{N} C_j^n \nabla^2 \phi_j(x_i, y_i) - \sum_{j=1}^{N} V_j^n \phi_j(x_i, y_i) \sum_{j=1}^{N} C_j^n \nabla \phi_j(x_i, y_i) + S_j \phi_j(x_i, y_i) \right] \tag{3}$$

where $i = 1, 2, \ldots, N_I$, where N_I denotes the total number of interior points and N denotes total number of points, V is velocity, C is species concentration, S is source or sink, Δt is the time step, superscript $n+1$ is the unknown value to be solved, μ is viscosity, D is the species diffusion coefficient, and superscript n is the current known value. The important point to illustrate here is that Eqs. (2-3) can be easily written and solved using any programming language. We have found that the use of MATLAB or MAPLE works very effectively, and is easy to implement.

Applications

Contaminant dispersion traces are affected by both the contaminant sources location and the indoor ventilation situations. Figure 1(a,b) shows particulate transport within a simple domain with ceiling ventilation and variable outflow boundary

conditions (door openings). The concentration exhausts into the ceiling vent with the right door closed. As the door is opened, the plume bends towards the door – this is due to the change in ventilation outflow.

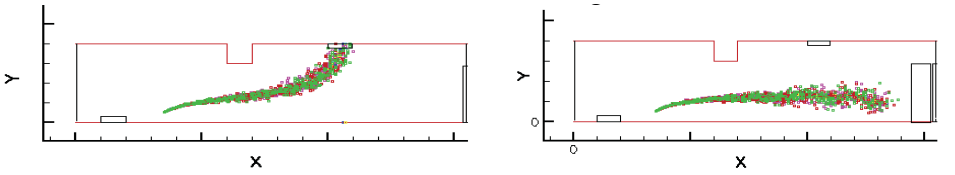

(a) exterior door closed (b) exterior door opened

Figure 1: Transport of particulates with exit door open and closed

Figure 2(a) shows the configuration of a two-room office complex [10]. Notice the different locations of contaminant sources denoted by the red dots. Particles are released from a pollutant source somewhere in the secretary's outer office. The meshless nodal configuration is shown in Fig. 2(b). Due to the door being opened, along with ventilation within the office complex (assumed in this case), the contaminant spreads into the inner office.

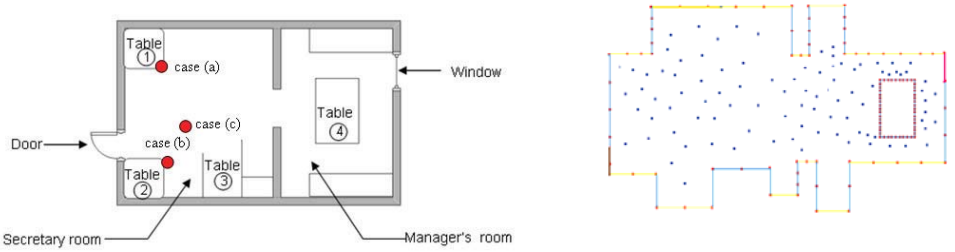

(a) Two-room office (b) meshless nodal pattern

Figure 2: Office complex layout

Figure 3(a,b) shows the particle paths within the two rooms. As can be seen from the particle dispersion patterns, the pollutant is transported and diffused by the ventilation pattern in the office complex. Source location is particularly important as the pollutant can travel to either side of the manager's desk within the inner office. When first responders arrive at an incident location, it is important that they be aware of the trajectory of the spreading contaminant. For example, the manager in the inner office should move to the lower right corner of his desk in case a (Fig. 3a), but should move to the upper left corner of his room in case b (Fig. 3b) until reached by a rescue team.

Contaminant dispersion within aircraft cabins is now being examined due to the increasing number of people traveling by airplane and the potential risk associated with exploding airborne contaminant. Sample seating map for an aircraft with 37

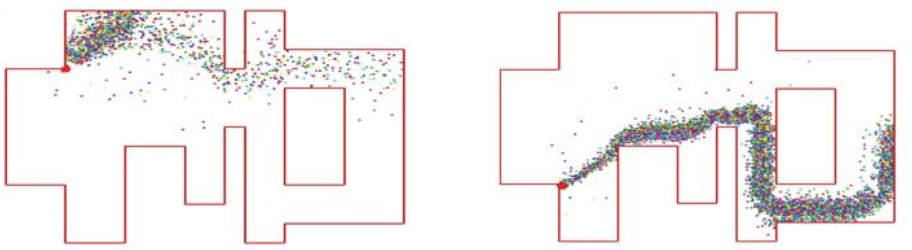

(a) Contaminant source in upper table (b) Contaminant source in lower table

Figure 3: Indoor particle dispersion within office: (a) upper table and (b) lower table

seats with one central aisle is shown in Fig. 4. One linear inlet is assumed in the ceiling of the cabin which supplies conditioned air to both sides of the cabin; the outlets are located at the floor level near the side walls.

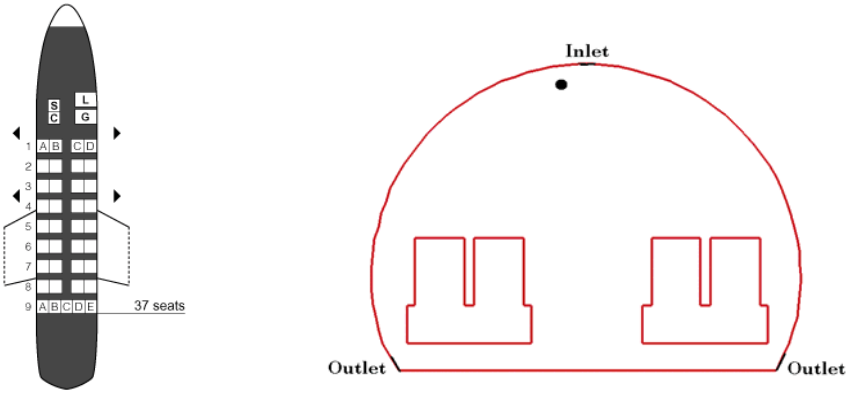

a) aircraft seating b) aircraft cross-section

Figure 4: Sample seating map and cross-section for aircraft

The cross-section for the cabin is shown in Fig. 4b. The inlet air entering the cabin is eventually extracted through the outlets. A hypothetical contaminant location is recognized as the dark dot – just slightly off cabin center. Storage bins or shelving near the ceiling were not included in this preliminary simulation. The meshless node pattern is shown in Fig. 5.

Model results are shown in Fig. 6(a, b) [12]. In this simulation, particles are introduced at the source location near the upper left ceiling of the cabin interior. The ventilation pattern symmetrically surrounds both sides of the aisle and eventually exits through the outlets beneath the seats, where higher velocity gradients develop as seen in Fig. 6(a). The particle dispersion pattern is clearly influenced by the ventilation pattern, as expected. In this instance, the particles (assuming they are slightly heavier than air) are advected and diffused into the aisle, then get primarily

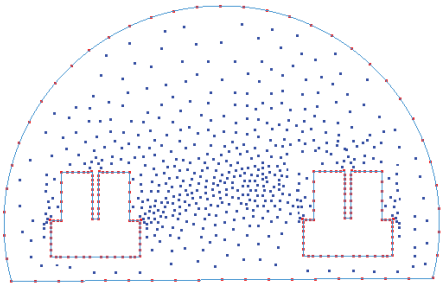

Figure 5: Meshless nodal pattern

swept under the seats to the left of the aisle (due to the asymmetric location of the source). Notice the dispersion of particles above the left seats, as opposed to none over the right seats – which is again a function of the source location. Infusion of contaminants directly into the ceiling inlet would create a more uniform dispersion pattern towards both sides of the cabin. A 3-D simulation is needed to ascertain the amount of contaminants moving in front of and behind the seats.

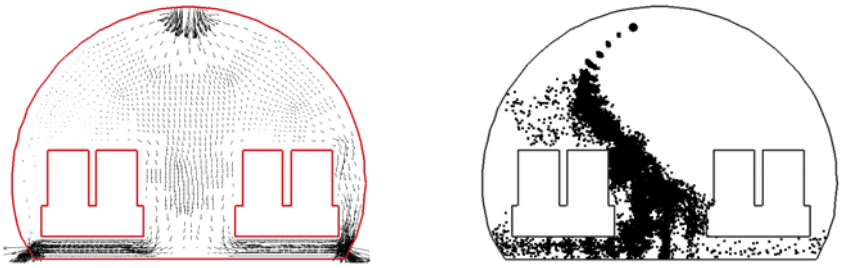

(a) Interior velocities

(b) Light particle dispersion traces

Figure 6: Cabin interior particulate dispersion

Conclusion

A meshless technique for simulating indoor air ventilation and contaminant dispersion has been developed. Preliminary results of different scenarios using the meshless numerical modeling approach with different contaminant sources (different in both contaminant particle size and locations) have been obtained for several indoor configurations.

Coupling sensors that would automatically trigger the model and set up appropriate response actions would allow immediate preventive measures to take affect. The model is well suited in building-related homeland security issues for prescribing contaminant exposure dispersion predictions and assessment related design and remediation studies. The model produces highly accurate results while requiring considerably less computer storage and CPU time than existing commercial CFD

codes. Development of a diffusion and transport database for different chemical and biological agents would be especially useful in assessment related design and making remediation policies.

References

1. Atluri, S.N. and Shen, S. (2002), "The meshless local Petrov-Galerking (MLPG) method: a simple & less-costly alternative to the finite element and boundary element method", *Computer Modelling in Engineering & Sciences*, Vol. 3, pp. 11-52.
2. Atluri, S. N. and D. W. Pepper (Eds.) (2002): *Advances in Computational Engineering & Science*, ICES '02, Reno, NV, July 31-Aug. 2.
3. Buhman, M.D. (2000), *Radial Basis Functions*, Cambridge University Press, Cambridge.
4. Chen, C. S., C. A. Brebbia, and D. W. Pepper (Ed.) (1999), *Boundary Element Technology XIII*, WIT Press, Southampton, UK, 708 p.
5. Chen, W. (2002), "New RBF collocation schemes and kernel RBFs with applications", *Lecture Notes in Computational Science and Engineering*, Vol. 26, pp. 75-86.
6. Franke, R. (1979), "A critical comparison of some methods for interpolation of scattered data", TR NPS-53-79-003, Naval Postgraduate School.
7. Hardy, R.L., (1971), "Multiquadric equations of topography and other irregular surfaces", *J. Geophy. Res*., Vol. 76, pp. 1905-1915.
8. Kansa, E.J (1990), "Multiquadrics – a scattered data approximation scheme with application to computational fluid dynamics, part I", *Computers and Mathematics with Applications*, Vol. 19, pp. 127-145.
9. Pepper, D. W. (2006), "Chapter 7: Meshless Methods," *Handbook of Numerical Heat Transfer*, 2nd Ed., W. J. Minkowycz et al (Eds.), John Wiley and Sons.
10. Pepper, D. W. and X. Wang (2007), "Modeling Indoor Contaminant Dispersion," *ICCES*, Vol. 1, No. 1, pp. 1-5.
11. Sarler, B. (2002), "Towards a mesh-free computation of transport phenomena", *Engineering Analysis with Boundary Elements*, Vol. 26, pp. 731-738.
12. Wang, X. and D. W. Pepper (2008), "A high-order numerical method for interior contaminant dispersion", 46^{th} AIAA Aerospace Sciences Meeting and Exhibit, Jan. 7 – 10, 2008, Reno, Nevada.
13. Kalla, N. D. and D. W. Pepper (2008), "A meshless radial basis function method for fluid flow with heat transfer", ICCES, Vol. 142, No. 1, pp. 1-6.